

## Lithographic Microfabrication for Nano/Micro-Objects by using Two-Photon Polymerization Technique

Kwang-Sup Lee,<sup>\*1</sup> Seung Wan Kang,<sup>1</sup> Ran Hee Kim,<sup>1</sup> Ju Yeon Kim,<sup>1</sup>  
Won Jin Kim,<sup>1</sup> Sang Hu Park,<sup>2</sup> Tae Woo Lim,<sup>2</sup> Dong-Yol Yang,<sup>2</sup>  
Hong-Bo Sun,<sup>3</sup> Satoshi Kawata<sup>3</sup>

<sup>1</sup>Department of Polymer Science and Engineering, Hannam University, Daejeon 306-791, Korea

<sup>2</sup>Department of Mechanical Engineering, Korea Advanced Institute of Science and Technology, Daejeon 305-701, Korea

<sup>3</sup>Department of Applied Physics, Osaka University, Suita, Osaka 565-0871, Japan

\*kslee@hannam.ac.kr

### Introduction

In the past few years, many studies of microscale fabrication technology using two-photon polymerization (TPP) induced with a femtosecond laser have been carried out [1-3]. TPP has many advantages as a technique for the direct fabrication of complex three dimensional (3D) structures on a scale of several microns, which are difficult to obtain using conventional miniaturization technologies. It is known that a femtosecond laser pulse can be closely focused onto liquid-state monomers and the resulting TPP used to initiate chemical processes and the formation of features close to 100 nm in size. A highly localized area around the center of the focused beam solidifies as a result of the absorption of the threshold energy for polymerization, the TPP rate is proportional to the square of the laser intensity. Therefore, a submicron to 100 nm resolution can be obtained using a high numerical aperture (NA) objective lens, with no restraints imposed by the diffraction limits of the beam. Liquid-state resins can be solidified by photopolymerization, i.e. by chain-growth polymerization reactions initiated by exposure to high intensity light. Current research into TPP is investigating the fabrication of precise 3D microstructures by utilizing various methodologies for specific applications [4]. To obtain micro-objects with high spatial resolution by making use of two-photon absorption (TPA) polymerization, efficient TPA chromophores are required as photosensitizers. Such materials have attracted particular attention in the field of 3D microfabrications with TPP technology because they enable the use of continuous wave (CW) lasers or nanosecond pulse lasers instead of expensive femtosecond lasers, but their use also improves microfabrication resolution. Thus research into the development of two-photon chromophores with high TPA cross-sections has been intense. In this presentation, the development through molecular engineering of highly efficient TPA materials that can be used in 3D microfabrications in the near infrared (NIR) regime, and also the development of various methods for improving the precision and efficiency of 3D microfabrications are reported.

### Experimental

For the fabrication of 3D microstructures with TPP, the nano-stereolithography (NSL) system illustrated in Figure 1 was developed. A mode-locked Ti:sapphire laser is used as the light source, providing a wavelength of 780 nm and a pulse width of less than 100 fs at a repetition rate of 80 MHz. The beam is scanned across the focal plane using a set of two Galvano-mirrors with a resolution of approximately 2.5 nm per step, and along the vertical axis using a piezoelectric stage. The laser is closely focused into a volume of photocurable resin with an objective lens that has a high numerical aperture (NA 1.25 or 1.4 x100, with immersion oil). A Galvano-shutter combined with a pin-holed plate is applied to obtain exposure times less than 1 ms. The pin-holed plate enables the interception of the beam (tilted by about one degree) to turn the laser beam on/off. The shutter, scanner, and piezoelectric stage are controlled using a control program. A high-magnification charge-coupled-device (CCD) camera is used for the optical adjustment of the focused beam and for monitoring the fabrication process.

To fabricate micro-objects with two-photon polymerization, the raster scanning method and the contour scanning method have both been utilized. In the raster scanning method, all of the cubic volume that contains the microstructure is scanned; in the contour scanning

method, the focused laser beam traces the contour profile of the microstructure. The contour scanning method requires less processing time and significantly increases the fabrication efficiency.

In the NSL process, one sliced layer of the 3D microstructure is solidified according to the scanning paths; another layer is fabricated after translating the location of the beam spot along the z-axis using the piezoelectric stage, which is then added to the previous solidified layers. The entire 3D structure is fabricated sequentially with this method. The 2D scanning paths of the focused laser beam for a given plane are obtained by using the intersection points between the slicing plane and the stereolithography (STL) data that are derived from 3-D CAD data; this method has been utilized widely in rapid prototyping processes.

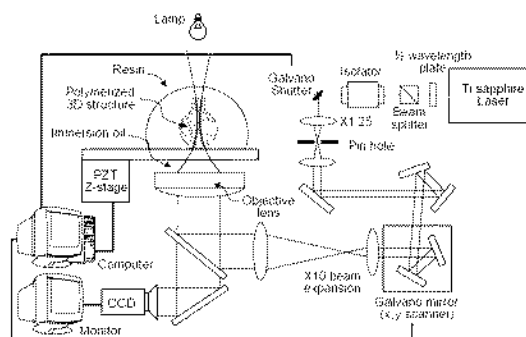


Figure 1. Schematic diagram of the 3D nano-stereolithography system.

### Results and discussion

**Efficient TPA Materials.** For symmetric linear centrosymmetric quadrupolar TPA molecules, the intramolecular charge transfer (ICT) character of the TPA molecule plays an important role in determining TPA activity, as shown by experimental and theoretical mechanistic studies into the nature of two-photon absorption. This can be clearly demonstrated with a theoretical treatment. According to the three-state model of the TPA process, the TPA cross-section,  $\delta$ , can be expressed as follows:

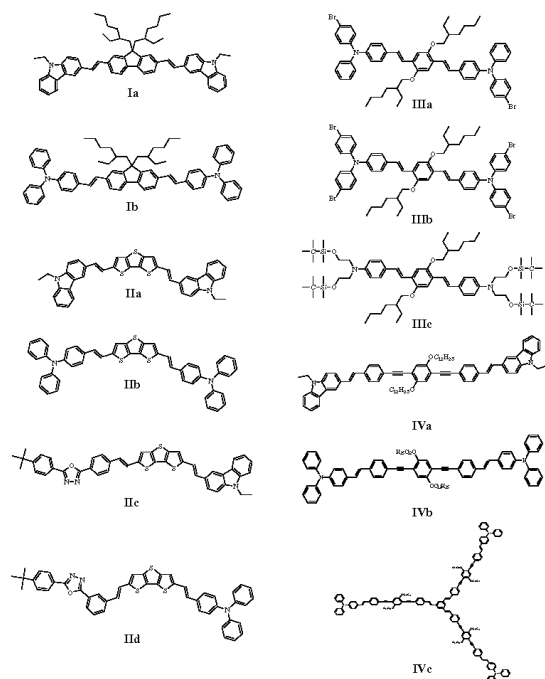
$$\delta \propto \frac{M_{01}^2 M_{12}^2}{(E_1 - E_0 - \hbar\omega)^2 \Gamma}$$

where the subscripts 0, 1, and 2 refer to the ground, one-photon excited, and two-photon excited states, respectively,  $E_n$  is the energy of state  $n$ ,  $M_{nm}$  is the transition dipole moment between states  $n$  and  $m$ , and  $\hbar\omega$  is the photon energy of the incident light. These parameters can be tuned to produce a large  $\delta$  by modifying the molecular structure so that  $(E_1 - E_0 - \hbar\omega)$  is reduced and  $M_{01}$  and  $M_{12}$  are increased. It is known that chain length extension results in an increase in  $M_{01}$ , whereas the introduction of donors at the ends or of  $\pi$ -bridges lead primarily to an increase in  $M_{12}$ . Thus the optical properties of TPA materials can be controlled by modulating both their core  $\pi$ -conjugation nature and their electron donor strength.

We have designed and prepared various types of TPA chromophores on the basis of this design concept for application in 3-D microfabrication with TPP. These chromophores can be classified according to their  $\pi$ -centers into three groups: i) fluorene derivatives (Ia-Ib), ii) dithieno[3,2-b;2',3'-d]thiophene (DTT) derivatives (IIa-IId), and iii) phenylenevinylene derivatives (IIIa-IIIc) and phenylene-ethynylene derivatives (IVa-IVc), as shown in Scheme 1. The two-photon induced fluorescence method using an fs-pulsed laser was employed for evaluation of their TPA activities. All these chromophores were found to exhibit high TPA activities. The electron donors in these chromophores were varied in the series of compounds I-IV to investigate the influence of donor strength on TPA activity.

Series I and II compounds have more delocalized  $\pi$ -cores such as fluorene and DTT; as shown in Table 1, these chromophores exhibit higher TPA activities than the series III based on phenylenevinylene moieties. There is little difference between the activities of the fluorene and DTT derivatives, except that they have different peak TPA cross-sections, in fluorene derivatives having triphenylamine and in DTT derivatives having carbazole. This indicates that the nature of the end group, donor strength and  $\pi$ -delocalization all contribute to the TPA response. Optical transparency of the TPA chromophores

Scheme 1. Molecular structures of two-photon absorbing materials



between 680 nm and 800 nm is essential for their application in microfabrications with two-photon photopolymerization, in order to avoid linear absorption by the TPA chromophore during TPP. These chromophores all exhibit no absorption above 500 nm (Table 1).

By comparing compounds I to IV, it becomes clear that TPA activity can be enhanced not only by introducing more delocalized and electron-rich  $\pi$ -centers, but also by symmetrically substituting strong electron donors at both ends. We also investigated the effects of inserting  $\pi$ -bridges between the  $\pi$ -centers and the electron donors by synthesizing various phenyleneethynylene derivatives (Scheme 1, IVa to IVc) and examining their TPA activities. It was found that the TPA cross-section values of this series peaked with that of the three-branched structure IVc ( $\sigma_2 = 5210 \text{ GM}$ ). This unexpected increase in TPA response may result from the cooperative effects of efficient  $\pi$ -delocalization and the concentrated volume due to its dendritic structure.

Table 1. Single-photon and two-photon photophysical parameters of TPA materials.

Dyes	$\lambda_{\text{max}}(\text{abs})$ (nm)	$\lambda_{\text{max}}(\text{PL})$ (nm)	$\Phi^a$	$\sigma^b$ (GM)	$\lambda_{\text{max}}(\text{TPA})$ (nm)
Ia	398	434	0.80	290 (80fs)	$\leq 735$
Ib	411	452	0.78	954 (80fs)	740
IIa	441	486	0.69	740 (80fs)	740
IIb	453	503	0.70	1140(80fs)	785
IIIa	424	507	0.81	470 (80fs)	780
IIIb	423 <sup>c</sup>	480 <sup>c</sup>	0.80	470(180fs)	780
IIIc	423 <sup>c</sup>	480 <sup>c</sup>	0.81	190 (80fs)	740
IVa	403	446	0.81	960 (80fs)	704
IVb	412	464	0.89	1184(80fs)	704
IVc	408	476	0.89	5219(80fs)	700

<sup>a</sup> Fluorescence quantum yield determined relative to fluorescein in 0.1 N NaOH.

<sup>b</sup> TPA cross-section; 1 GM =  $10^{-50} \cdot \text{cm}^4 \cdot \text{s} \cdot \text{photon}^{-1}$  measured in two-photon fluorescence method

<sup>c</sup> Solution in  $\text{CH}_2\text{Cl}_2$  and the others are THF solution.

**Precise 3D microfabrications by the TPP.** For the nano-patterning with high spatial resolution, understanding the performance of individual voxels is also critical. We found that at near-threshold exposure condition voxel shape scaling follows different laws by means of varying laser power and changing exposure time. The aspect ratio of vertical and lateral lengths of a voxel, when exposure gets

stronger, it monotonically increases and reaches a saturation status for the two processes, that are conventionally regarded as equivalent for voxel volume tuning. Based on this finding, they were able to produce the voxels with a near 100-nm lateral spatial resolution at the optimized condition. In addition, by employing two-photon polymerization at low laser power and short period of exposure time, We have successfully fabricated a wide variety of two-dimensional and three-dimensional photonic and micro-devices with high resolution as show in Figure 2. Such success implies that it is possible to accomplish the manufacturing that is otherwise not accessible. Further it can develop into opening of new scientific and technological possibility in nano and micro research.

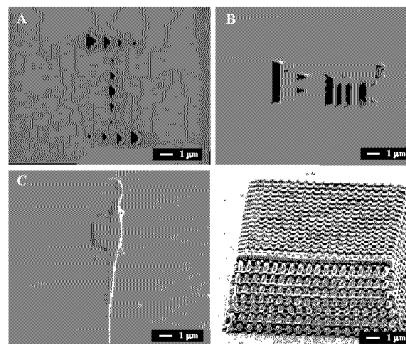


Figure 2. SEM images of various 2D and 3D micro-patterns fabricated by the two-photon-induced polymerization; (A, B) 2-D patterns of voxels and letters, (C, D) 3-D patterns of a lizard sculpture and photonic lattice.

Due to the intrinsic 3D processing capability of TPP, it has been utilized in the fabrication of 3D photonic crystals. However, most efforts to fabricate photonic crystals are frustrated except in limited cases by the occurrence of the no band gap effect in laser-written structures. This phenomenon is hindering the development of state-of-the-art laser nanofabrication technology and its widespread use in photonic crystal research and applications.

In an attempt to solve this problem, we employed a shape precompensation technique [4] with TPP. After the developing process for removing the remaining liquid resins with several ethanol drops, woodpile structures were found to shrink linearly due to inevitable deformations in the microstructures. The lateral linear shrinkage rate in a unit length is  $2\%/\mu\text{m}$  along the substrate normal direction. The structural deformation in the transition layer is detrimental to high-precision microfabrication, particularly for optoelectronic devices. In order to compensate for the effects of this undesirable phenomenon, it was found that by considering the shrinkage rate, the anticipated shape and size disparity could be corrected at the stage of structure design. The effectiveness of the resulting writing schemes of photonic crystals was evidenced by the photonic band gap effect that is half an order stronger than those reported. We observed the intensity rejection of 81% in the transmission valley at  $5120 \text{ cm}^{-1}$ .

In addition, we also developed various techniques for fabricating precision 3D patterns by the double contour scanning, top-down reverse patterning, and subregional slicing [5-7]. From the results of recent progress in TPP techniques, it is predicted that TPP will fulfill its promise as a leading 3D nanofabrication technology because of its intrinsic advantages.

## References

- [1] Cumpston, B.H.; Perry, J.W.; et.al. *Nature* **1999**, *398*, 51.
- [2] Sun, H-B.; Kawata, S. *Adv. Polym. Sci.* **2004**, *170*, 169.
- [3] Lee, K.-S.; Yang, D.-Y.; Park, S.H.; Kim, R.H. *Polym. Adv. Tech.*, **2006**, *17*, 72.
- [4] Sun, H-B.; Suwa, T.; Takad, K.; Zaccaria, R.P.; Kim, M.-S.; Lee, K.-S.; Kawata, S. *Appl. Phys. Lett.* **2004**, *85*, 370.
- [5] Park, S. H.; Lim, T.W.; Yang, D.-Y.; Kong, H.J.; Kim, J.Y.; Lee, K.-S. *Macromol. Res.*, **2006**, *14*, 245.
- [6] Park, S. H.; Lee, S.H.; Yang, D.-Y.; Kong, H.J.; Lee, K.-S.; *Appl. Phys. Lett.*, **2005**, *87*, 154108.
- [7] Park, S. H.; Lim, T.W.; Yang, D.-Y.; Jeong, J.-H.; Kim, K.-D.; Lee, K.-S.; Kong, H.J. *Appl. Phys. Lett.*, **2006**, *88*, 203105.